Noname manuscript No.
(will be inserted by the editor)

Observing *Thermobifida fusca* Cellulase Binding to Pretreated Wood Particles Using Time-Lapse Confocal Laser Scanning Microscopy
Supplemental Material

Paul Zhu · Jose M. Moran-Mirabal · Jeremy S. Luterbacher · Larry P. Walker · Harold G. Craighead

Received: date / Accepted: date

Theory of Experiment

*Transient Enzyme-Binding Model*In enzyme-catalyzed reactions, the first step is for enzyme E and substrate S to form an enzyme-substrate complex ES before a product P is produced and a free enzyme released and again becomes available for reaction (Nelson and Cox 2004). In the case of cellulose hydrolysis, cellulase adsorption to cellulose has been studied in depth to determine the rate-limiting step. Langmuir model was first proposed by Peitersen *et al* to describe the relationship between free and adsorbed cellulase (Peitersen et al. 1997). As a result of fast enzyme-substrate adsorption, most of the theoretical work has used steady-state enzyme concentrations to determine the binding kinetics (Lee et al. 1982; Stiner et al. 1988; Stuart and Ristroph 1985). It can be shown however, when observation intervals can be made fast compared to reaction times, transient kinetics can be measured directly, and parameters extracted from a transient model (Johnson 2005).

In symbolic form, an enzyme-catalyzed reaction can be represented by,

$$E + S \underset{k_{-1}}{\overset{k_1}{\rightleftharpoons}} ES \underset{k_{-2}}{\overset{k_2}{\rightleftharpoons}} E + P$$

P. Zhu · H.G. Craighead (✉)
Applied Engineering & Physics
Cornell University
Ithaca, NY, 14853
Tel: +1-607-255-6286
Fax: +1-607-255-7658
E-mail: hgc1@cornell.edu

J.M. Moran-Mirabal · L.P. Walker
Biological & Environmental Engineering
Cornell University
Ithaca, NY, 14853

J.S. Luterbacher
Chemical & Biomolecular Engineering
Cornell University
Ithaca, NY, 14853

where k_1 is binding rate, k_{-1} unbinding rate, and k_2 is the rate at which product P is formed from the ES complex, k_{-2} the reverse production rate. If the concentrations of E, S and P, denoted subsequently using square brackets, have the unit $mol \cdot L^{-1}$ or M, then k_1 and k_{-2} have the unit $M^{-1} \cdot min^{-1}$, k_{-1} and k_2 have the unit min^{-1}. Clearly the concentrations $[E]$, $[S]$ and $[P]$ depend on time t.

In cases where there is negligible reaction producing P, for example slow cellulose hydrolysis at room temperature, and only enzyme adsorption forming ES complexes, the above equation simplifies to

$$E + S \underset{k_{-1}}{\overset{k_1}{\rightleftharpoons}} ES$$

When an immobilized substrate with surface binding site concentration $[S(t)]$ is immersed in enzyme solution at concentration $[E(t)]$, the rate of change in the surface concentration of enzyme-substrate complex $[ES(t)]$ is described by

$$\frac{d[ES(t)]}{dt} = k_1[E(t)][S(t)] - k_{-1}[ES(t)]$$

with initial condition $[ES(0)] = 0$.

Assuming a large reservoir of enzyme solution, the enzyme concentration $[E(t)]$ stays constant throughout the time frame of interest. Therefore its time dependence is subsequently dropped for clarity. The available substrate concentration at any time t is $[S(t)] = [S^M] - [ES(t)]$, where $[S^M]$ is the maximum concentration of available binding sites on the substrate. The differential equation can be rearranged and written as

$$\frac{d[ES(t)]}{dt} = k_1[E][S^M] - (k_1[E] + k_{-1})[ES(t)]$$

This equation can be solved (Kusse and Westwig 1998) to yield the following solution:

$$[ES(t)] = \frac{k_1[E][S^M]}{k_1[E] + k_{-1}}(1 - e^{-(k_1[E]+k_{-1})t}) \tag{1}$$

which agrees with a solution obtained by Johnson (Johnson 2005). Defining the dissociation constant $K_d = k_{-1}/k_1$, and allowing $t \to \infty$, the Langmuir binding isotherm,

$$[ES] = \frac{[E][S^M]}{[E] + K_d}$$

is obtained.

*Spectra Separation*Since the rate of fluorescently-labeled cellulase binding to immobilized substrates was inferred from the observed fluorescence increase, it was essential to separate label fluorescence from other fluorescence sources. In many cases, careful selection of fluorescence emission filters is adequate in discriminating different emission sources, giving excellent qualitative, if not quantitative, description of fluorophore distribution (Murphy et al.). However, spectral deconvolution is needed to obtain meaningful numerical values of fluorophore concentration. Knowing the spectral shape of each fluorochrome in the system, and knowing the photon collector response to the rise of fluorescence signal (the simplest being a linear response), fluorophore concentration can be back-calculated from collected photons. Consequently, binding coefficients can be estimated from the rate of change in collected fluorescence signal.

When measuring fluorescence in bulk, the collected fluorescence intensity I^{PMT} by a photo multiplier tube (PMT) is a function of excitation light intensity I^{EX}, number of fluorophores n in the focal volume, the average extinction coefficient σ of each fluorophore, quantum yield ϕ^f of the fluorophore, collection efficiency of the optical system η, transmission properties of the emission band-pass filter T^{BP}, and quantum yield ϕ^{PMT} of the PMT, written as,

$$I^{PMT} = I_{EX} \cdot \sigma \cdot n \cdot \phi^f \cdot \eta \cdot T^{BP} \cdot \phi^{PMT}$$

Fluorescence is the emission of a photon during electronic transition from the first excited singlet state to the ground singlet state after optical excitation. The photon energy is equal to the difference between the lowest vibrational level of the excited state and the vibrational level of the singlet ground state (Masters and So 2008). Therefore the emission spectrum of a fluorophore does not depend on the number of its species, n, or the intensity of the excitation beam. In other words, maintaining a constant physical environment of the fluorophore results in a constant σ and ϕ^f. For a given excitation light intensity I^{EX}, the collected fluorescene intensity for each optical system set up (i.e, same objective, filter set, etc) is written as,

$$I^{PMT} = \alpha \cdot n$$

where

$$\alpha = I^{EX} \cdot \sigma \cdot \phi^f \cdot \eta \cdot T^{BP} \cdot \phi^{PMT}$$

If there are two species of fluorophores n_1 and n_2, being illuminated simultaneously, and their fluorescence collected by two photon collection channels, separated by distinct emission band-pass filters, each PMT observes an intensity given by

$$\begin{bmatrix} I_1^{PMT} \\ I_2^{PMT} \end{bmatrix} = \begin{bmatrix} \alpha_{11} & \alpha_{12} \\ \alpha_{21} & \alpha_{22} \end{bmatrix} \cdot \begin{bmatrix} n_1 \\ n_2 \end{bmatrix} \triangleq \mathbf{A} \cdot \begin{bmatrix} n_1 \\ n_2 \end{bmatrix}$$

where we have defined the cross-talk matrix $\mathbf{A}$ that completely describes the distribution of fluorescence signal from each fluorophore species into either photon collection channels. Each matrix coefficient α_{ij} is

$$\alpha_{ij} = I^{EX} \cdot \sigma_j \cdot \phi_j^f \cdot \eta_i \cdot T_{ij}^{BP} \cdot \phi_i^{PMT}$$

where i denotes collection channel number, and j a fluorophore species. Since each fluorophore's emission spectrum covers a range of wavelengths, depending on the bandpass filter used in each optical path, the off-diagonal elements of $\mathbf{A}$ may not vanish, which results in signal bleed-through.

To accurately discern the number of bound enzymes, it is necessary to determine each individual element α_{ij} and calculate the number n_j from I_i^{PMT} using the relationship

$$\begin{bmatrix} n_1 \\ n_2 \end{bmatrix} = \mathbf{A}^{-1} \cdot \begin{bmatrix} I_1^{PMT} \\ I_2^{PMT} \end{bmatrix}$$

Commercially available software can perform spectral deconvolution with known fluorophores and system set up. With uncharacterized fluorophores or a custom optical system, it is necessary to measure α_{ij}. To find α_{11} and α_{21}, I_1^{PMT} and I_2^{PMT} are measured with a known n_1 while n_2 is set to 0. α_{12} and α_{22} can be found in similar fashion with known n_2 and holding $n_1 = 0$. This method can be easily expanded into multi-channel, multi-fluorophore system, as long as $\mathbf{A}$ is not singular.

Materials and Methods

*Microscope coverslip preparation*Four-inch $170\mu m$ borosilicate wafers were first patterned with gold fiducial marks and cut into $16 \times 16mm^2$ square cover slips. Techniques of lithographically defining gold patterns on dielectric substrate have been described elsewhere (Ilic et al. 2004). After acetone and isopropyl alcohol rinses, and O_2 plasma clean (Harrick Plasma, Ithaca, NY), a coverslip was glued to the bottom of a MatTek (Ashland, MA) $35mm$ petri dish, covering the $14mm$ pre-fabricated opening. The MatTek petri dish held the cellulase solution during binding experiments.

*Immobilization of Pretreated Wood Particles*A drop of $10\mu L$ water suspension containing approximately $0.01\%(w/w)$ of pretreated particles was pipetted on the gold-patterned coverslip, covering approximately an area of $60mm^2$. The surface was allowed to dry overnight at ambient temperature, to let particles adhere. The adsorbed particles were rehydrated with $50mM$ sodium acetate buffer ($pH = 5.5$) and the borosilicate surface was washed 3 times, with gentle agitation (Orbital shaker at 60 rpm for 5 min each). The particles were then incubated with 0.5% Bovine Serum Albumin (BSA) in $2mL$ sodium acetate buffer for 30 min, before being washed again and incubated in sodium acetate buffer over night, ready for imaging. Normally at this point, over 90% of particles would have been washed away. Yet the remaining dozen or so particles were sufficient for time-lapse enzyme-binding experiments.

*Scanning Electron Microscopy (SEM) Imaging of Immobilized Particles*To study the surface morphology of individual particles, SEM was used to take high-resolution images of immobilized particles. A clean borosilicate substrate, along with immobilized particles, was first coated with approximately 20Å gold-palladium using a Hummer V sputtering tool (Technics, San Jose, CA), at a pressure of $39mTorr$, sputtering current $10mA$, for approximately 30 s. The resulting metal film coating helps dissipate the charge that can build up when a dielectric sample, such as pretreated wood, is targeted under an electron beam. SEM images were taken with a Zeiss Ultra 55 (Carl Zeiss NTS GmbH, Oberkochen, Germany), at an accelerating voltage of $1.38kV$, aperture size of $30\mu m$, and a working distance $2.6mm$.

*Confocal Laser Scanning Microscope (CLSM) Set Up*See Fig. 1

*CLSM Characterization*To determine the range of fluorescent signals that could be safely taken without saturating photo detectors, the CLSM was characterized using Alexa Fluor 488-5'-dUTP and Alexa Fluor 647-5'-dUTP (Molecular Probes, Eugene OR) at various concentrations. From these measurements shown in Fig. 2, it was determined that for a 12-bit image with maximum pixel value of 4095, pixel intensities below 3500 were linearly related to fluorephore concentration (Rost 1991). Such linear relationship is a necessary condition for spectral deconvolution using matrix transformation.

For our system, the cross-talk matrix used in spectral deconvolution was found to be:

$$\mathbf{A} = \begin{bmatrix} 0.87 & 0.14 & 0 \\ 0.13 & 0.52 & 0 \\ 0 & 0.34 & 1 \end{bmatrix}$$

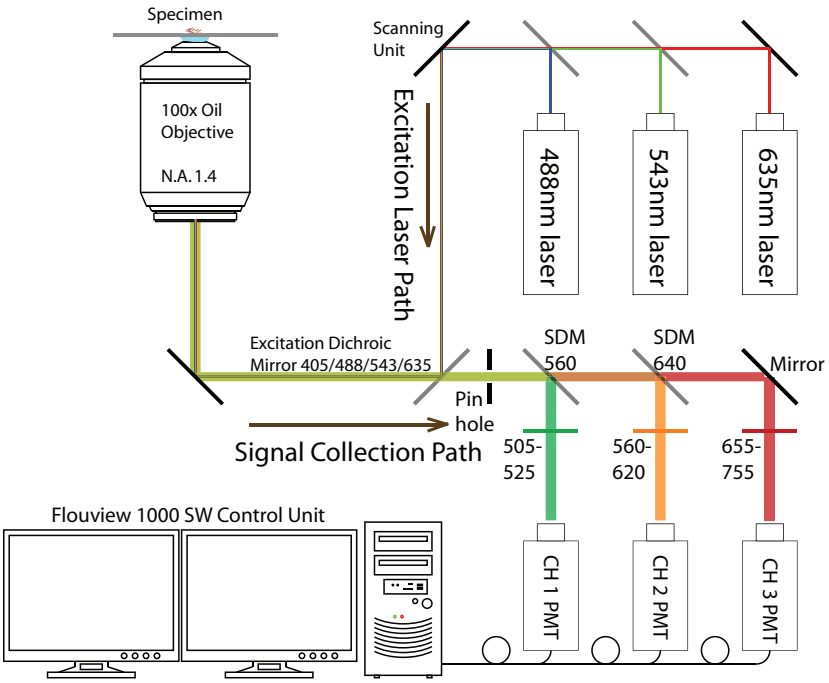

Fig. 1 Confocal Laser Scanning Microscope set up using Olympus Flouview 1000 system. Excitation lasers at 488nm, 543nm and 635nm are combined and scanned to illuminate the specimen through a SAPO 100x Oil objective with Numerical Aperture (N.A.) of 1.4. Fluorescence signal is collected with the same objective, and passed through a sequence of single band dichroic mirrors (SDM), filtered with band-pass optical filters before being collected by the photo-multiplier tubes (PMT) of each channel (CH)

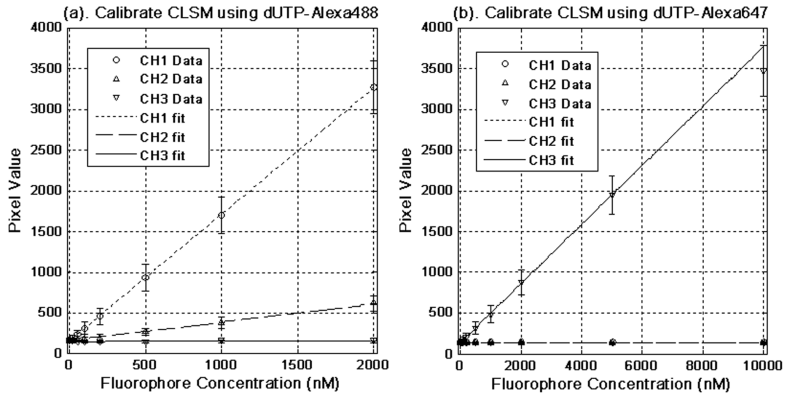

Fig. 2 Determining linear range of CLSM system by imaging (a) 5'-dUTP-Alexa 488 and, (b) 5'-dUTP-Alexa 647 fluorophores at concentrations between 20nM and 10μM, with excitation lasers at 488nm, 543nm and 635nm all set at 2% of their respective maximum power levels. For a 12-bit image, pixel intensities of less than 3500 are seen linearly correlated with fluorophore concentration, validating the requirement for linear transformation used in spectral separation

*Data Processing*Custom MATLAB (The Mathworks, Natick, MA) routines were used to perform numerical spectra separation and curve fitting of fluorescence intensity data to the

binding model. Specifically, time-lapse images saved by Fluoview software were first combined into one intensity map, showing highest fluorophore concentration areas, which were selected as regions of interest (ROI). Five discrete ROIs were cropped out of each intensity map, and used as masks to generate time-series intensity averages of each respective ROI. Intensity data from three color channels were run through linear transformation routine to generate actual fluorescence profiles of AF488, AF647, and wood autofluorescence, respectively. And finally, time-trace of AF488 or AF647 were fitted to enzyme binding-kinetics model to obtain binding coefficients. Out of each set of experiment using a labeled enzyme at certain concentration, between 20 and 30 ROIs were analyzed to obtain binding coefficients, from which an average and standard deviation were calculated.

*Effect of ROX Buffer*As mentioned before, ROX buffer was used to improve photon output and photostability. To determine the rate of loss of fluorescence at nominal illumination laser power (2%), a piece of pretreated wood particle was allowed to incubate in ROX buffer with $2.5nM$ Cel6B labeled with AF488, and $2.5nM$ Cel6B labeled with AF647, for 6 hours at room temperature. A small area of a particle was then continuously imaged and the collected fluorescence monitored. The saved images were fed through spectra separation routine, and intensities of autofluorescence, AF488, and AF647 were extracted. The intensity time traces were fitted to an exponential decay function, giving the per-scan fluorescence decay rates.

The oxygen scavenging cocktail has different effects on the autofluorescence of wood, and on the fluorescence of AF488 and AF647. The per-scan decay rates of AF488 and autofluorescence of wood were approximately 0.2%, so small that they can be safely ignored for all practical purposes. On the other hand, AF647 had a slightly higher rate of fluorescence decrease, at approximately 0.8% per laser scan. Depending on the number of images taken, this attenuation factor may need to be taken into account. However for this study, the uncertainty due to diverse morphologies in the pretreated wood particle overwhelmed the slight decrease in AF647 fluorescence. Therefore this factor was ignored as well. For comparison, similar bleaching experiments were carried out with $5mM$ ascorbic acid in sodium acetate buffer, in place of ROX buffer. Comparable bleaching characteristics were observed for AF488 and wood autofluorescence. However, the bleaching rate for AF647 fluorophores was approximately twice as fast as that in ROX buffer. Additionally, in comparing temporal fluorescence increase data taken using enzyme in ROX buffer to that in buffer with ascorbic acid, no significant difference in binding rates was observed (data not shown). Therefore no observable adverse effect was imposed by ROX buffer on cellulase binding.

References

Ilic B, Craighead H, Krylov S, Senaratne W, Ober C, Neuzil P (2004) Attogram detection using nanoelectromechanical oscillators. J Appl Phys 95:3694–3703

Johnson KA (2005) Enzyme kinetics: Transient phase. In: Encyclopedia of Life Sciences, John Wiley & Sons, Ltd.

Kusse B, Westwig E (1998) Mathematical Physics. Wiley Interscience

Lee SB, Shin HS, Ryu DDY, Mandels M (1982) Adsorption of cellulase on cellulose effect of physicochemical properties of cellulose on adsorption and rate of hydrolysis. Biotechnology and Bioengineering 24:2137–2153

Masters BR, So P, eds. (2008) Handbook of Biomedical Nonlinear Optical Microscopy. Oxford University Press

Murphy DB, Piston DW, Shand SH, Watkins SC, Davidson MW () Spectral bleed-through artifacts in confocal microscopy. URL http://www.olympusfluoview.com/theory/bleedthrough.html

Nelson DL, Cox MM (2004) Lehninger Principles of Biochemistry. Fourth ed., W.H. Freeman and Company

Peitersen N, Medeiros J, Mandels M (1997) Adsorption of trichoderma cellulase on cellulose. Biotechnology and Bioengineering 19(7):1091–1094

Rost F (1991) Quantitative Fluorescence Microscopy. Cambridge University Press

Stiner W, Sattler W, Esterbauer H (1988) Adsorption of *Trichoderma reesei* cellulase on cellulose: Experimental data and their analysis by different equations. Biotechnology and Bioengineering 32:853–865

Stuart JY, Ristroph DL (1985) Analysis of cellulose-cellulase adsorption data: A fundamental approach. Biotechnology and Bioengineering 27:1056–1059